The $(1\times1)\rightarrow$hexagonal structural transition on Pt(100) studied by high-energy resolution core level photoemission

Alessandro Baraldi,[a] Erik Vesselli, Laura Bianchettin, and Giovanni Comelli
Physics Department and Center of Excellence for Nanostructured Materials, Trieste University, Via Valerio 2, I-34127 Trieste, Italy Laboratorio TASC INFM-CNR, S.S. 14 Km 163.5, I-34012 Trieste, Italy

Silvano Lizzit and Luca Petaccia
Sincrotrone Trieste S.C.p.A., S.S. 14 Km 163.5, I-34012 Trieste, Italy

Stefano de Gironcoli
SISSA—Scuola Internazionale Superiore di Studi Avanzati and INFM-CNR DEMOCRITOS National Simulation Center via Beirut 2-4, I-34014 Trieste, Italy

Andrea Locatelli, T. Onur Mentes, and Lucia Aballe
Sincrotrone Trieste S.C.p.A., S.S. 14 Km 163.5, I-34012 Trieste, Italy

Jonas Weissenrieder
MAX-lab, Lund University, Box 118, S-221 00 Lund, Sweden

Jesper N. Andersen
Department of Synchrotron Radiation Research, Lund University, Box 118, S-221 00 Lund, Sweden

(Received 20 March 2007; accepted 12 September 2007; published online 22 October 2007)

The $(1\times1)\rightarrow$quasihexagonal (HEX) phase transition on a clean Pt(100) surface was investigated by monitoring the time evolution of the Pt4$f_{7/2}$ core level photoemission spectra. The spectral component originating from the atoms forming the (1×1) metastable unreconstructed surface was found at -570 ± 20 meV with respect to the bulk peak. *Ab initio* calculations based on density functional theory confirmed the experimental assignment. At temperatures above 370 K, the (1×1) phase irreversibly reverts to the more stable HEX phase, characterized by a surface core level shifted component at -185 ± 40 meV. By analyzing the intensity evolution of the core level components, measured at different temperatures in the range of 393–475 K, we determined the activation energy of the phase transformation, $E=0.76\pm0.04$ eV. This value is considerably lower than the one previously determined by means of low energy electron diffraction. Possible reasons for this discrepancy are discussed. © *2007 American Institute of Physics*.
[DOI: 10.1063/1.2794344]

I. INTRODUCTION

Among the transition metals surfaces, Pt(100) represents an intriguing case for the remarkable differences in chemical reactivity between the (1×1) unreconstructed phase and the reconstructed high-temperature quasihexagonal phase (HEX). A vast literature has therefore been dedicated to the structural determination of the different phases,[1–3] the mechanism of reconstruction[4,5] (also in the presence of adsorbates), and the understanding of chemical properties, related in particular to the oscillatory behavior of a large number of surface chemical reactions.[6]

Similar to other (100) 5*d* transition metal surfaces such as Ir and Au, Pt exhibits a quasihexagonal reconstructed stable phase, periodically matching the (100) substrate. Different symmetries of the first and the subsurface layers result in a large (5×25) unit cell. Scanning tunneling microscopy (STM) clearly revealed that the topmost layer has a hexagonal structure, characterized, however, by a large-scale height modulation. Due to a contraction of the Pt–Pt distance, the topmost layer accommodates about 25% more atoms than the bulk-terminated ideal (100) layer. Density functional theory (DFT) calculations[4] have identified the tensile excess stress of the unreconstructed (1×1) phase, originating from a *d* charge depletion in the surface layer, as the driving mechanism for the formation of the reconstructed phase. The HEX reconstruction can be lifted by adsorbates such as CO,[7–14] NO,[15–19] and O,[20–27] as the gain in adsorption energy overcompensates the loss in reconstruction energy. The transition from the (1×1) to HEX phase has also been invoked to interpret the oscillatory kinetics of a large number of chemical reactions on Pt, as due to periodical switching between two states of different catalytic activity. In these studies, $CO+O_2$, $NO+CO$, $NO+H_2$, and $NO+NH_3$ chemical reactions have been widely studied[6] in the attempt to develop a mathematical model describing the oscillatory chemical reactivity. In general this involves the definition of a set of coupled differential equations, describing the variation of the adsorbate coverage on the HEX and (1×1) phases and the phase transition between the two. In this context, one of the most important parameters is the activation energy of the

[a]Author to whom the correspondence should be addressed. Electronic mail: alessandro.baraldi@elettra.trieste.it

$(1\times1)\rightarrow$HEX structural transition, which quantifies the thermal stability of the (1×1) phase.

While for the Au(100) surface a mechanism was proposed based on atomic migration from steps or islands (which act as sources of the 25% excess HEX surface atoms), a different mechanism has recently been suggested for the Pt(100) $(1\times1)\rightarrow$HEX phase transition, based on the presence of an intermediate phase.[5] This process involves the extraction of extra atoms from the second layer, forming subsurface vacancies. The effective activation energy E_a for the subsurface vacancy creation has been estimated to be 1.2 eV (pre-exponential factor of 10^{13} s^{-1}), slightly larger than the unique experimental value reported so far, obtained by low energy electron diffraction measurements which is 0.91 eV.[28]

In the present paper, we investigate the transition from the (1×1) to the HEX phase on Pt(100) by means of high-energy resolution core level photoemission. The time evolution of Pt4$f_{7/2}$ spectra measured at different temperatures allows us to determine the activation energy of the process. Differences between our experimental findings and previously reported activation energies for the same process are discussed.

II. EXPERIMENTAL

The photoemission studies were performed at the I311 beamline of the third generation synchrotron radiation source MAX II, Lund, Sweden.[29] The background pressure in the main chamber was always better than 1×10^{-10} mbar. The Pt(100) single crystal was cleaned by Ar ion sputtering at room temperature ($E=1.2$ keV), annealing to 1250 K, oxygen cycles in order to remove residual carbon (in the temperature range of 570–1070 K at $p_{O2}=1\times10^{-7}$ mbar), and finally, hydrogen reduction to remove residual oxygen traces ($p_{H2}=1\times10^{-7}$ mbar, $T=470-770$ K). Surface cleanness was checked by inspecting the C1s, Si2p, S2p, and O1s signals. The overall energy resolution (beamline+spectrometer) of the Pt4$f_{7/2}$ spectra was 50 meV at the photon energies we used, ranging from 120 to 150 eV. Core level binding energies (BE) have always been calibrated with respect to the Fermi level.

The metastable (1×1) clean layer is prepared with a procedure similar to the one developed by Kuhnke *et al.*[30] using He diffraction. NO is based at 300 K ($p_{NO}=2\times10^{-8}$ mbar) for about 600 s, monitoring in real time the N1s signal evolution. It is well known that in the saturated NO layer the reconstruction is completely lifted. The surface is then annealed to 420 K in an oxygen atmosphere ($p=1\times10^{-7}$ mbar) in order to desorb part of the NO layer and allow the residual NO to dissociate, thus forming a chemisorbed oxygen layer on a (1×1) substrate (N immediately leaves the surface as N_2 after NO dissociation). The resulting surface is completely covered by chemisorbed oxygen as evidenced by the O1s signal and the absence of a N1s signal. After cooling to 340 K the oxygen is removed by low pressure hydrogen reduction at 2×10^{-9} mbar, monitoring the O1s signal and stopping the hydrogen flux as soon as all oxygen has been reacted off, in order to minimize residual hydrogen on the surface. The high-photon flux of the beamline allows measurement of the O1s intensity evolution with high surface sensitivity [better than 0.1% of monolayer (ML)] and time resolution (10 s/spectrum). Small traces of residual hydrogen (less than 1%) can be easily desorbed by 2–3 flashing cycles below 420 K (~10 K/s), a temperature at which HEX-induced diffraction spots start to be observed in a slow heating process (0.06 K/s).[30]

Low energy electron microscopy (LEEM) and micro-low-energy-electron-diffraction (LEED) were used to provide a local characterization of the surface structure. These microscopic investigations were done using the spin polarized LEEM (SPLEEM) microscope available at the Nano-Spectroscopy beamline at ELETTRA.[31]

The core level photoemission spectra were fitted with a Doniach-Šunjić (DS) function,[32] characterized by the singularity index parameter α (final-state screening of the core hole) and by the Lorentzian width Γ (finite core-hole lifetime), convoluted with a Gaussian of width G, which takes into account the broadening due to the phonons, the surface inhomogeneity, and the instrumental resolution. A linear background was also subtracted.

III. DFT CALCULATIONS

The core level binding energies were calculated using a density functional theory based formalism[33,34] employing the generalized gradient approximation[35,36] as implemented in the Quantum-ESPRESSO open source distribution.[37] The interaction between the electrons and the ionic cores is described by an ultrasoft pseudopotential.[38] The Kohn-Sham equations are solved self-consistently using a plane-wave basis set restricted to a kinetic energy cutoff of 32 Ry. In order to deal with the metallic character of the system and to improve the convergence with respect to the number of k points of the Brillouin zone integration the contribution from each k point is broadened by using a Methfessel and Paxton smearing function[39] of order 1 with a width $\sigma=0.012$ Ry.

For the (1×1) cell a sampling with a $(10\times10\times2)$ Monkhorst-Pack grid was adopted, resulting in 15 special k points in the irreducible wedge.[40] The Pt(100) surface was modeled by a fully relaxed seven-layer slab with a vacuum region corresponding to five interlayer spacings, enough to avoid interactions between neighboring slabs as previously found.[41] Final state core level binding energies can be accurately computed in the pseudopotential formalism we used by describing the excited atom by a pseudopotential generated in the core-excited configuration. In this formulation the core level binding energies, including final state effects, are given by the pseudopotential total energy difference supplemented by an additive constant that can be determined for the isolated atom and cancel out when computing binding energy differences. Initial state contributions can also be extracted by a frozen-density calculation. The estimated absolute error in the surface core level shift is ±30 meV. Details of the method we used can be found in Ref. 41.

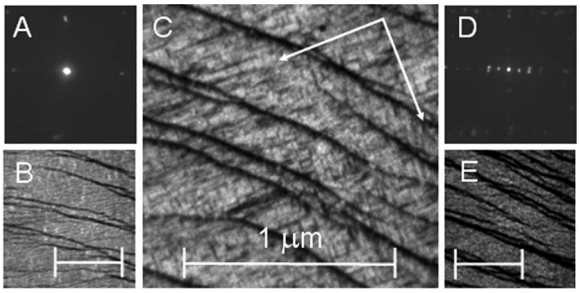

FIG. 1. (a) (1×1) LEED of the deconstructed surface (E=70 eV). The corresponding LEEM image (E=16 eV) (b) demonstrates the homogeneous lateral development of the (1×1) phase; step and step bunches appear darker than the terraces. (c) Development of needlelike HEX domains during annealing of the (1×1) phase (T=420 K, E=6 eV); main crystallographic axes are indicated by the white arrows. (d) LEED of the HEX reconstructed surface (E=55 eV) and (e) corresponding LEEM image (E=16 eV). In all LEEM images the white bar indicates a length of 1 μm.

IV. RESULTS AND DISCUSSION

A. Surface Characterization

The deconstructed surface displays a good (1×1) LEED pattern [Fig. 1(a)]. LEEM [Fig. 1(b)] shows no structural contrast, which is direct evidence for the laterally homogeneous distribution of the (1×1) phase. Phase contrast in the images reveals instead a complex surface morphology. Typically, large flat areas with densely spaced single steps (average terrace width of 40 nm) and a few step bunches are observed.

LEEM is ideally suited to follow the dynamics of the phase transition occurring during annealing of the (1×1) metastable structure. At an electron energy of 6 eV it is possible to obtain structural contrast between the (1×1) and the HEX phases, the latter appearing brighter than the (1×1) as seen in Fig. 1(c). Typically, the HEX phase grows in needlelike domains which are preferentially aligned along the main crystallographic directions and can extend up to $\sim300\times50$ nm^2. With increasing time (or temperature), the HEX phase tends to cover the entire surface [Figs. 1(d) and 1(e)].

The growth mode of the HEX phase during annealing of the (1×1) phase mirrors is observed during the inverse process. In fact, when the HEX reconstruction is lifted by NO adsorption, the (1×1) domains have similar asymmetric shape and orientation. This is in agreement with previous scanning tunneling microscopy (STM) experiments and simulations for the CO-induced lifting of the HEX,[7] which demonstrated that the surface restructures via the ejection of chains of Pt atoms. Our LEEM data (not shown) indicate that the same mechanism can determine the shape of the domains up to mesoscopic length scales.

Prior to the phase transition measurements, we independently characterized the (1×1) and HEX phases. In Fig. 2 the Pt4$f_{7/2}$ spectrum of the clean (1×1) structure measured at 90 K and 120 eV photon energy is shown, together with the individual components resulting from the data analysis. Only two peaks (A and B) were used to fit the spectrum at 71.02 and 70.45 eV, respectively, i.e., with a core level shift of 570±20 meV. Best fits were obtained with two DS functions with different values of the fitting parameters

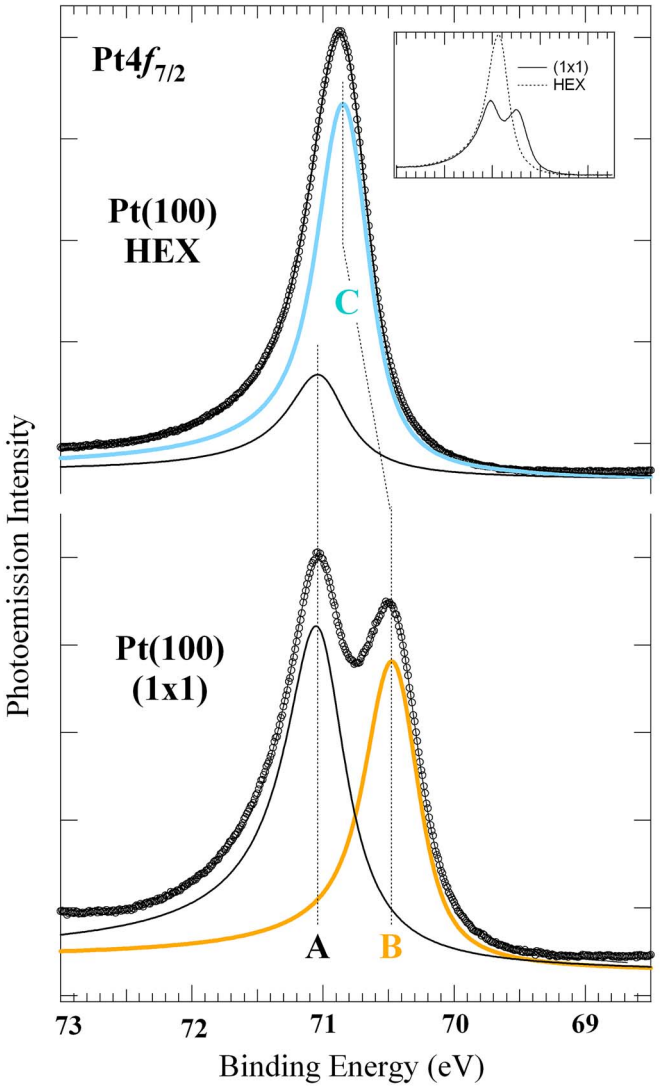

FIG. 2. (Color online) Pt4$f_{7/2}$ core level spectra corresponding to (1×1) and HEX phases measured at 90 K and 120 eV photon energy (spectra are plotted on a different scale, see inset). The (1×1) spectrum can be fitted by two components corresponding to bulk (A) and first-layer (B) atoms with a surface core level shift of −570 meV. For simplicity, also the HEX phase has been fitted by considering only one surface component (C) at −180 meV with respect to the bulk peak.

(Γ_A=480 meV, Γ_B=310 meV, α_A=0.14, α_B=0.13, G_A=100 meV, and G_B=240 meV). In order to determine the origin of these components we first acquired Pt4$f_{7/2}$ spectra at high photoelectron kinetic energies (above 300 eV). The low binding energy component B presents a reduced intensity, as expected for a surface component, due to the increased inelastic electron mean free path. In addition, the lower binding energy component is strongly modified by small traces of adsorbates such as oxygen and hydrogen, deliberately dosed on the clean surface at room temperature. Finally, for a 5d transition metal surface with a d-band more than half occupied, the surface peak is expected to have a smaller binding energy with respect to the bulk peak, with a shift that, in absolute value, should be even larger than the one found for the close-packed Pt(111) surface, i.e., −400 meV.[42–44]

In order to simplify the fitting procedure, the spectrum

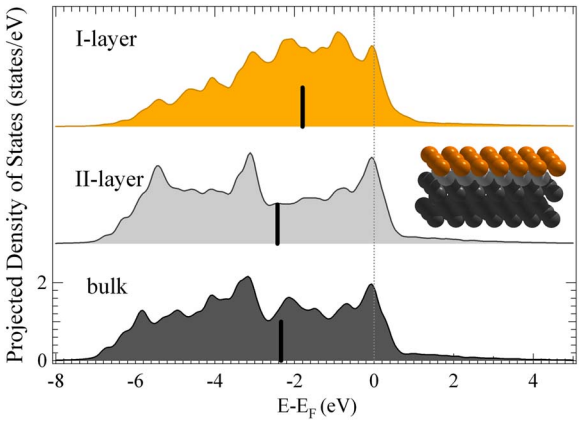

FIG. 3. (Color online) Density of states projected onto the 5*d* orbitals of the Pt atoms in the inequivalent configurations of the (1×1) unreconstructed phase (see insert): bulk (black), second-layer (gray), and first-layer surface atoms (orange). The calculated atom-projected *d*-band center is also reported.

corresponding to the HEX phase has also been fitted with a single surface component, whose lineshape parameters were fixed to the values of the (1×1) surface component. Although this clearly represents a strong approximation, as first-layer atoms involved in the (5×25) structure are geometrically slightly inequivalent, the alternative solution would require that an unreasonable number of components was included in the fitting procedure.

It should be noted that the overall integrated intensity of the HEX peak is about 32% larger than (1×1)-related peak, as clearly visible in the inset of Fig. 2. This can be ascribed to the higher surface atomic density, even though photoelectron diffraction effects at these photoelectron kinetic energies can be relevant. For the same reason we could also explain the decreased intensity of the bulk component in the HEX spectrum. On the basis of all the above considerations, we assign the lower BE component to first-layer Pt atoms. In order to support these conclusions by means of a quantitative comparison with the experimental findings, we performed DFT calculations of the Pt(100) surface core level shift for the unreconstructed structure.

The fully relaxed (1×1) surface shows a first-to-second layer distance which is contracted by 2.4% with respect to the calculated bulk interlayer spacing of 1.99 Å. The equilibrium geometry is in very good agreement with previous theoretical results which yielded a surface relaxation of −2.6%.[45] Furthermore, our density functional theory (DFT) calculations confirm the experimental assignment of the lower BE component, since the calculated surface core level shift is −510±30 meV.

There is still a small discrepancy between the theoretical and measured values. As second-layer contributions have been found[46] to be important in Rh(100) and Rh(111) surfaces for a detailed comparison between experimental and theoretical spectra, in order to asses the impact of such effect in the present case, we also calculated the second-layer subsurface core level shift. Indeed we found a small positive shift (+22 meV) in the second-layer contribution with respect to the bulk peak, consistent with the fact that second-layer atoms have a somewhat higher coordination than the

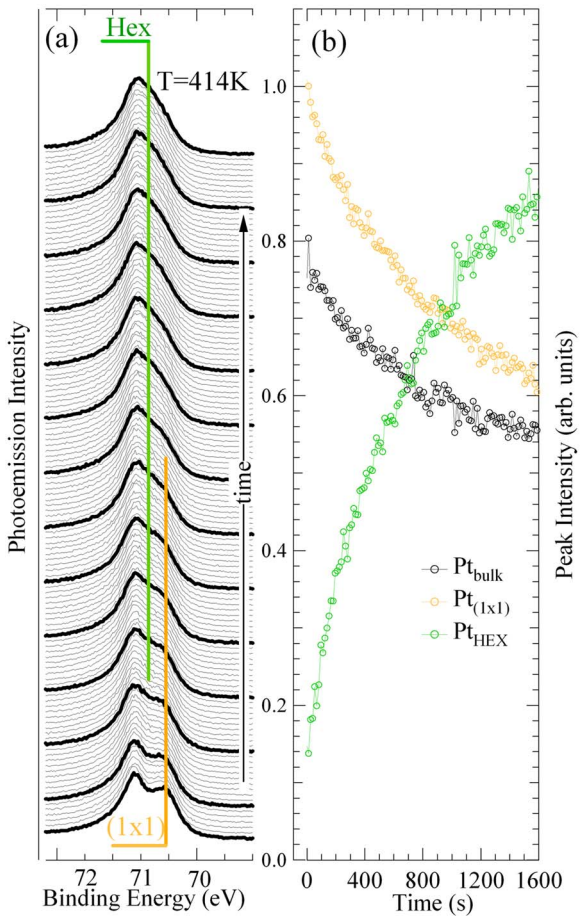

FIG. 4. (Color online) (a) Time evolution of the Pt4$f_{7/2}$ core level spectra measured at T=414 K and $h\nu$=120 eV. Each spectrum was measured in 14 s. The yellow line indicates the position of the (1×1)-related surface core level component, while the green line indicates the binding energy of the HEX-induced surface core level shifted peak. (b) Intensity evolution of the three peaks' integrated areas (black=bulk, green=HEX, yellow=1×1) versus time, obtained by fitting the sequence of about 130 spectra, recorded at constant temperature.

bulk one, due to the reduced first-to-second layer distance.[46] Accounting for this minor shift in the experiment would bring experimental and theoretical results in even closer agreement. We did not, however, add a new core level component so close to the bulk peak in the data analysis for two reasons: (i) it is known that, as for Pd,[47] the DS lineshape does not accurately describe the Pt4*f* profile, due to the rapid change of the density of states around the Fermi level, and (ii) the LEEM images show the presence of step bunches and thus not only first-layer but also second-layer atoms with coordination $n\neq12$ are expected, resulting in other low intensity core level components hidden underneath the bulk peak.

On Pt(100), the Pt4$f_{7/2}$ surface core level shift appears to be dominated mainly by initial state effects due to the reduced coordination of surface atoms, as the calculated contribution from the electronic core hole screening is about +70 meV for both first- and second-layer atoms. This is clearly visible in Fig. 3, where the calculated partial density of states[48] of first-layer, second-layer, and bulk atoms is plotted. The displacement[49] of the *d*-band center of the surface atoms with respect to the bulk ones, $\Delta B_d=B_d^{\mathrm{bulk}}-B_d^{\mathrm{surf}}$, goes

for the clean (1×1) structure from −541 meV in the case of the first-layer atoms to +90 meV for second-layer atoms.

B. KINETICS

The identification of the surface core level shifted components permits the study of the kinetics of the (1×1) structural transformation to the HEX phase. The time evolution of the intensity of the (1×1)-related component as a function of time at different temperatures ranging from 393 to 475 K is a measure of the changes in the population of (1×1)-type atoms. The same approach has been previously applied to study the thermal stability of the Rh(110) $(1\times n)$ missing-row reconstruction.[50] Figure 4(a) shows a typical sequence of Pt4$f_{7/2}$ spectra acquired at 414 K (acquisition time ~14 s/spectrum). Already a qualitative inspection of the evolution of the raw data reveals that the high binding energy component at 70.80 eV, ascribed to atoms in the HEX configuration, grows with time, while the (1×1) related surface component gradually disappears.

The intensity versus time curves are plotted in Fig. 4(b): initially the intensity of the (1×1)-surface component decays exponentially, while the HEX surface component grows with time. Also the bulk peak intensity diminishes, as expected by comparing HEX and (1×1) low temperature spectra. The results for the time evolution of the (1×1)-related peak at different temperatures are summarized in Fig. 5. The curves seem to follow an exponential decay with a decay constant τ that decreases with increasing temperature. However, in the whole temperature range spanned by our experiment, this behavior applies only at the early stages of the transition and it is important to note that a complete transition to the HEX phase takes place only at very high temperatures. Indeed, even at 475 K, i.e., the highest temperature studied, the (1×1)-induced component does not disappear completely. Since the $(1\times1)\rightarrow$HEX transition is an activated process, assuming that the rate follows an Arrhenius equation, we fitted the initial time evolution with the $A\exp(-t\tau)$ function, where the rate τ is $\nu\exp(-E_A/k_BT)$, E_A is the energy barrier of the process, ν is the pre-exponential factor, and k_B is the Boltzman constant.

Each series of spectra measured at a different temperature was fitted using three components, with DS lineshape, repeating the analysis several times with the Gaussian lineshape parameters and the BE positions of the different core level components fixed at several values, until the minimal chi-square for the whole series was found. This procedure was adopted in order to take into account the possible contribution of first-to-second layer expansion and phonon-induced broadening effects, yielding a reliable estimate of the τ error bar parameter in the Arrhenius plot reported in Fig. 6. The activation energy value derived is 0.76±0.04 eV.

Even if the results are not in disagreement considering the error bars, the activation energy we found is considerably lower than the value of 0.91±0.17 eV previously reported by means of low energy electron diffraction.[28] This would imply a transition rate difference at the lower temperature (T=373 K) of about two orders of magnitude.

However, as suggested by He diffraction measurements,[30] the preparation method of the metastable (1×1) reported in Ref. 28 and used in other experimental investigations to prepare the metastable (1×1) phase[52,53] results in small traces of atomic hydrogen in the sample (around 5% of ML), which can influence the phase transition. For instance, these He diffraction measurements[30] demonstrated that a small residual H coverage (below 10%) stabilizes the (1×1) phase up to more than 400 K.

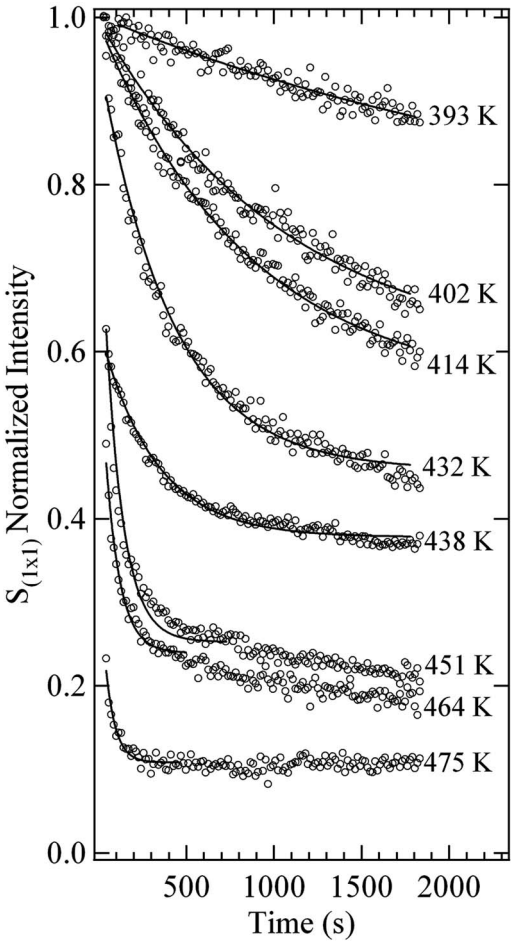

FIG. 5. Time evolution of the integrated intensity of the (1×1)-related Pt4$f_{7/2}$ surface core level component measured in the 393–475 K temperature range. All the intensities have been normalized to the surface component intensity measured at room temperature. Continuous lines represent the fit with the function $A\exp(-t\tau)$.

Indeed it is well known that adsorbates can promote or inhibit atomic surface diffusion. Using STM Horch *et al.*[54] studied the hydrogen-promoted self-diffusion process of platinum adatoms deposited on the (1×2) missing-row reconstructed phase of Pt(110). In that case, DFT calculations showed that the Pt–H complex consisted of a hydrogen atom trapped on top of a platinum atom, placed in the trough along the $[1\bar{1}0]$ direction, resulted in a 0.09 eV reduction of the diffusion barrier, in good agreement with the experimental finding of 0.16 eV. On the contrary, for a (1×1)-Pt(100) surface prepared by the field evaporation technique, Kellogg showed that chemisorbed hydrogen inhibits the exchange displacement diffusion mechanism of Pt adatoms.[55] Mobile hydrogen atoms, sitting next to the Pt adatom, increase the diffusion barrier by enhancing the energy required to remove

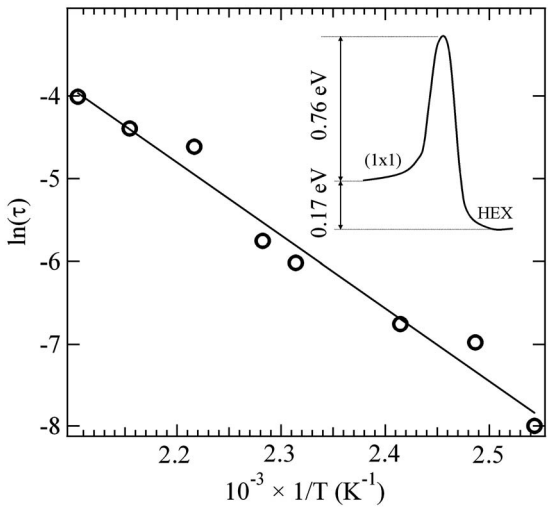

FIG. 6. Arrhenius plot of the rate of the restructuring process obtained from the data in Fig. 5. Inset shows a schematic energy diagram illustrating the clean $(1\times1)\rightarrow$HEX structural transition, with initial and final state energy values obtained by the calorimetric measurements of Yeo *et al.* (Ref. 51) and with the energy barrier determined in this work.

a surface atom from the substrate. In recent theoretical investigations, based on DFT and molecular dynamics simulations,[5,45] the mechanism of atom extraction from the second layer creating subsurface vacancies is the process proposed as the first step for the formation of the HEX phase starting from the metastable (1×1) structure. We therefore conclude that the higher activation energy value previously obtained using LEED can be ascribed to the presence of residual traces of atomic hydrogen left by a non-optimized preparation procedure.

As mentioned above, the intensity evolution is exponential only initially, most probably a sign of the existence of a different, competing mechanism for the transformation of the (1×1) towards the HEX phase. As found by Van Beurden *et al.* in MD simulations,[5] besides the homogeneous vacancy formation process, two other heterogeneous processes are expected. The first one involves a reconstruction process, which initiates at step edges, where each second atomic row on the surface shifts half an atomic distance along the [011] direction. In the second one, step edges and island corners get dissolved by absorption into surface layers. Both mechanisms, which would require a large mass transport from the steps over the surface, are associated with defects and are expected to proceed at a lower rate than the subsurface vacancy mechanism.

V. CONCLUSION

By monitoring the time evolution of the Pt4$f_{7/2}$ core level photoemission spectra we have studied the $(1\times1)\rightarrow$quasihexagonal (HEX) phase transformation on Pt(100). We have shown that the (1×1) phase, showing a surface core level shifted component at −570 meV, irreversibly reverts to the HEX phase, characterized by a component at −185 meV, at temperatures above 370 K. The analysis of the intensity evolution of the core level components, measured in the range of 393–475 K, allowed us to determine the activation energy of the phase transformation, $E=0.76\pm0.04$ eV, which results to be considerably lower than the one previously determined by means of LEED. The difference is explained as due to residual hydrogen in the LEED measurements.

ACKNOWLEDGMENTS

We acknowledge financial support by the MIUR under the program FIRB 2003 and the Swedish Research Council. Calculations were performed at SISSA and at the CINECA computing center, also thanks to INFM-CNR computing grants.

The MAX-lab staff is gratefully acknowledged for technical assistance.

[1] J. J. Mortensen, T. R. Linderoth, K. W. Jacobsen, E. Lægsgaard, I. Stensgaard, and F. Besenbacher, Surf. Sci. **400**, 290 (1998).
[2] G. Ritz, M. Schmid, P. Varga, A. Borg, and M. Rønning, Phys. Rev. B **56**, 10518 (1997).
[3] A. Borg, A. M. Hilmen, and E. Bergene, Surf. Sci. **306**, 10 (1994).
[4] V. Fiorentini, M. Methfessel, and M. Scheffler, Phys. Rev. Lett. **71**, 1051 (1993).
[5] P. van Beurden and G. J. Kramer, J. Chem. Phys. **121**, 2317 (2004).
[6] R. Imbihl and G. Ertl, Chem. Rev. (Washington, D.C.) **95**, 697 (1995) and references therein.
[7] P. Van Beurden, B. S. Bunnik, G. J. Kramer, and A. Borg, Phys. Rev. Lett. **90**, 66106 (2003).
[8] R. J. Behm, P. A. Thiel, P. R. Norton, and G. Ertl, J. Chem. Phys. **78**, 7437 (1983).
[9] T. E. Jackman, K. Griffiths, J. A. Davies, and P. R. Norton, J. Chem. Phys. **79**, 3529 (1983).
[10] M. Kim, W. S. Sim, and D. A. King, J. Chem. Soc., Faraday Trans. **92**, 4781 (1996).
[11] R. J. Behm, P. A. Thiel, P. R. Norton, and G. Ertl, Surf. Sci. **121**, L553 (1982).
[12] R. J. Behm, P. A. Thiel, P. R. Norton, and G. Ertl, J. Chem. Phys. **78**, 7448 (1983).
[13] A. Hopkinson, X.-C. Guo, J. M. Bradley, and D. A. King, J. Chem. Phys. **99**, 8262 (1993).
[14] A. Hopkinson, J. M. Bradley, X.-C. Guo, and D. A. King, Phys. Rev. Lett. **71**, 1597 (1993).
[15] Y. Y. Yeo, L. Vattuone, and D. A. King, J. Chem. Phys. **104**, 3810 (1996).
[16] K. Mase and Y. Murata, Surf. Sci. **242**, 132 (1991).
[17] P. Gardner, M. Thushaus, R. Martin, and A. M. Bradshaw, Surf. Sci. **240**, 112 (1990).
[18] G. Pirug, H. P. Bonzel, H. Hopster, and H. Ibach, J. Chem. Phys. **71**, 593 (1979).
[19] M. Gruyters, A. T. Pasteur, and D. A. King, J. Chem. Soc., Faraday Trans. **92**, 2941 (1996).
[20] J. M. Bradley, A. Hopkinson, and D. A. King, J. Chem. Phys. **99**, 17032 (1995).
[21] J. A. Davies, T. E. Jackman, D. P. Jackson, and P. R. Norton, Surf. Sci. **109**, 20 (1981).
[22] E. Lang, W. Grimm, and K. Griffiths, J. Vac. Sci. Technol. A **2**, 1028 (1984).
[23] K. Griffiths, T. E. Jackmann, J. A. Davies, and P. R. Norton, Surf. Sci. **138**, 113 (1984).
[24] G. Kneringer and F. P. Netzer, Surf. Sci. **49**, 125 (1975).
[25] P. R. Norton, K. Griffiths, and P. E. Bindner, Surf. Sci. **138**, 125 (1984).
[26] R. B. Shumbera, H. H. Kan, and J. F. Weaver, Surf. Sci. **600**, 2928 (2006).
[27] A. A. Deskins, J. Lauterbach, and K. T. Thompson, J. Chem. Phys. **122**, 184709 (2005).
[28] P. R. Norton, J. A. Davies, D. K. Creber, C. W. Sitter, and T. E. Jackman, Surf. Sci. **108**, 205 (1981).
[29] R. Nyholm, J. N. Andersen, U. Johansson, B. N. Jensen, and I. Lindau, Nucl. Instrum. Methods Phys. Res. A **467**, 320 (2001).
[30] K. Kuhnke, K. Kern, and G. Comsa, Surf. Sci. **343**, 44 (1995).
[31] A. Locatelli, L. Aballe, T. O. Mentes, M. Kiskinova, and E. Bauer, Surf.

Interface Anal. **38**, 1554 (2006).
[32] S. Doniach and M. Šunjić, J. Phys. C **3**, 185 (1970).
[33] P. Hohenberg and W. Kohn, Phys. Rev. **136**, 864 (1964).
[34] W. Kohn and L. Sham, Phys. Rev. **140**, 1133 (1965).
[35] J. P. Perdew, in *Electronic Structure of Solids '91*, edited by P. Ziesche and H. Eshring (Akademie, Berlin, 1991), p. 11.
[36] J. P. Perdew, K. Burke, and M. Ernzerhof, Phys. Rev. Lett. **77**, 3865 (1996).
[37] S. Baroni, S. de Gironcoli, A. Dal Corso, and P. Giannozzi, http://www.quantum-espresso.org.
[38] D. Vanderbilt, Phys. Rev. B **41**, 7892 (1990).
[39] M. Methfessel and A. T. Paxton, Phys. Rev. B **40**, 3616 (1989).
[40] H. J. Monkhorst and J. D. Pack, Phys. Rev. B **13**, 5188 (1976).
[41] L. Bianchettin, A. Baraldi, S. de Gironcoli, S. Lizzit, L. Petaccia, E. Vesselli, G. Comelli, and R. Rosei, Phys. Rev. B **74**, 45430 (2006).
[42] O. Björneholm, A. Nilsson, H. Tillborg, P. Bennich, A. Sandell, B. Hernäs, C. Puglia, and N. Mårtensson, Surf. Sci. **315**, L983 (1994).
[43] C. Puglia, A. Nilsson, B. Hernnäs, O. Karis, P. Bennich, and N. Mårtensson, Surf. Sci. **342**, 119 (1995).
[44] J. F. Zhu, M. Kinne, T. Fuhrmann, R. Denecke, and H. P. Steinruck, Surf. Sci. **529**, 384 (2003).
[45] P. Van Beurden, "On the Surface Reconstruction of Pt-Group Metal," Ph.D. Thesis, Eindhoven University of Technology, 2003.
[46] A. Baraldi, L. Bianchettin, S. de Gironcoli, E. Vesselli, S. Lizzit, L. Petaccia, G. Zampieri, G. Comelli, and R. Rosei, New J. Phys. **9**, 143 (2007).
[47] S. Surnev, M. Sock, M. G. Ramsey, F. P. Netzer, M. Wiklund, M. Borg, and J. N. Andersen, Surf. Sci. **470**, 171 (2000).
[48] The partial density of states is defined as the projection of the density of states onto the atomic wave function ϕ_i^{at}: $n_i=\Sigma_n\int_{\mathrm{BZ}}\delta(E-E_n(\mathbf{k}))|\langle\phi_i^{\mathrm{at}}|\psi_n(\mathbf{k})\rangle|^2d\mathbf{k}$, where $\psi_n(\mathbf{k})$ is the crystal wave function of the nth band at wave vector $\mathbf{k}$.
[49] We define the pth moment of the density of states $n_i(E)$ as $\mu_p=\int\varepsilon^p n_i(\varepsilon)d\varepsilon$; μ_0 and μ_1/μ_0 give the total number of states in the band and the center of gravity position B_d, respectively.
[50] A. Baraldi, S. Lizzit, F. Bondino, G. Comelli, R. Rosei, C. Sbraccia, N. Bonini, S. Baroni, A. Mikkelsen, and J. N. Andersen, Phys. Rev. B **72**, 75417 (2005).
[51] Y. Y. Yeo, C. E. Wartnaby, and D. A. King, Science **268**, 1731 (1995).
[52] H. P. Bonzel, G. Broden, and G. Pirug, J. Catal. **53**, 96 (1978).
[53] P. R. Norton, J. A. Davies, D. K. Creber, C. W. Sitter, and T. E. Jackman, Surf. Sci. **108**, 205 (1981).
[54] S. Horch, H. T. Lorensen, S. Helveg, E. Lægsgaard, I. Stensgaard, K. W. Jacobsen, J. K. Nørskov, and F. Besenbacher, Science **398**, 134 (1999).
[55] G. L. Kellogg, Phys. Rev. Lett. **79**, 4417 (1997).